Respiratory Physiology & Neurobiology 260 (2019) 37–52

Contents lists available at ScienceDirect

Respiratory Physiology & Neurobiology

journal homepage: www.elsevier.com/locate/resphysiol

The contribution of endogenous glutamatergic input in the ventral respiratory column to respiratory rhythm

Denise R. Cook-Snyder[a], Justin R. Miller[b], Angela A. Navarrete-Opazo[c], Jennifer J. Callison[c], Robin C. Peterson[a], Francis A. Hopp[d], Eckehard A.E. Stuth[c,e], Edward J. Zuperku[c,d], Astrid G. Stucke[c,e,*]

[a] Department of Neuroscience, Carthage College, Kenosha, WI, United States
[b] Department of Biology, Carthage College, Kenosha, WI, United States
[c] Department of Anesthesiology, Medical College of Wisconsin, Milwaukee, WI, United States
[d] Zablocki VA Medical Center, Milwaukee, WI, United States
[e] Children's Hospital of Wisconsin, Milwaukee, WI, United States

ARTICLE INFO

Keywords:
Glutamatergic disfacilitation
Ventral respiratory column
Respiratory rhythm
Bötzinger Complex
preBötzinger Complex
Reciprocal inhibition

ABSTRACT

Glutamate is the predominant excitatory neurotransmitter in the ventral respiratory column; however, the contribution of glutamatergic excitation in the individual subregions to respiratory rhythm generation has not been fully delineated. In an adult, in vivo, decerebrate rabbit model during conditions of mild hyperoxic hypercapnia we blocked glutamatergic excitation using the receptor antagonists 2,3-dihydroxy-6-nitro-7-sulfamoyl-benzo[f]quinoxaline-2,3-dione (NBQX) and d(–)-2-amino-5-phosphonopentanoic acid (AP5). Disfacilitation of the preBötzinger Complex caused a decrease in inspiratory and expiratory duration as well as peak phrenic amplitude and ultimately apnea. Disfacilitation of the Bötzinger Complex caused a decrease in inspiratory and expiratory duration; subsequent disfacilitation of the preBötzinger Complex resulted in complete loss of the respiratory pattern but maintained tonic inspiratory activity. We conclude that glutamatergic drive to the preBötzinger Complex is essential for respiratory rhythm generation. Glutamatergic drive to the Bötzinger Complex significantly affects inspiratory and expiratory phase duration. Bötzinger Complex neurons are responsible for maintaining the silent expiratory phase of the phrenic neurogram.

1. Introduction

The preBötzinger Complex (preBötC) region in the ventral respiratory column (VRC) contains all neuron types necessary to generate a respiratory rhythm. Several hypotheses have been put forth regarding the generation of inspiratory (I) phase activity. The "group-pacemaker hypothesis" proposes that glutamatergic pre-inspiratory (pre-I) neurons with endogenous bursting properties mutually excite each other and other inspiratory neurons resulting in cyclic inspiratory activity (Funk and Greer, 2013). In vitro recordings of preBötC neuron and field potentials and hypoglossal nerve activity suggested that low-amplitude "burstlets" that chronologically appear before high-amplitude, respiratory pattern generating inspiratory bursts may represent this pre-I activity (Kam et al., 2013). Tonic synaptic input to these pre-I neurons is required for regular bursts (Butera et al., 1999). In this model, the duration and amplitude of the inspiratory cycle is limited by inhibitory inputs, at least in part derived from somatostatin-positive post-inspiratory neurons within the preBötC, which have been characterized by Cui et al. (Cui et al., 2016). These neurons may be different from the expiratory decrementing (E-dec) neurons described by Ezure in the preBötC and Bötzinger Complex (BötC), which discharge throughout the entire expiratory phase (Ezure, 1990). The relevance of the BötC region for rhythm generation in this model remains under debate (Bongianni et al., 2010; Janczewski et al., 2013; Marchenko et al., 2016).

A competing model proposes that transition from expiratory to inspiratory phase involves the decreasing inhibition of I-driver neurons, which usually show pre-I activity (Lindsey et al., 1987; Rybak et al., 2008), and I-decrementing (I-dec) neurons by E-decrementing (E-dec) neurons (Ezure, 1990). As inhibition decreases later in the expiratory phase, the inspiratory neurons become spontaneously excitable. A self-reexcitatory network of I-driver, pre-I neurons and I-augmenting (I-aug) neurons produces synchronous inspiratory bursts and also excites I-dec neurons, which inhibit E-dec and E-augmenting (E-aug) neurons in the

* Corresponding author at: Department of Anesthesiology, Medical College of Wisconsin, 8700W Watertown Plank Road, Milwaukee, WI, 53201, United States.
E-mail address: astucke@mcw.edu (A.G. Stucke).

https://doi.org/10.1016/j.resp.2018.11.011
Received 25 September 2018; Received in revised form 22 November 2018; Accepted 25 November 2018
Available online 28 November 2018
1569-9048/ © 2018 Elsevier B.V. All rights reserved.

BötC and caudal ventral respiratory group (cVRG). Disfacilitation of pre-I neurons and decreasing I-dec inhibition of E-dec neurons results in termination of the inspiratory and beginning of the expiratory phase. Both models include reexcitation among inspiratory neurons and assume tonic excitatory drive to the area.

The exact nature of respiratory drive to the subareas of the VRC has not been fully elicited. Central chemodrive is mostly generated by chemoreceptive neurons of the Retrotrapezoid Nucleus (RTN), which contains chemoreceptive, tonically discharging neurons (Mulkey et al., 2004), and has glutamatergic projections to all respiratory-related areas of the pons and VRC (Bochorishvili et al., 2012; Mulkey et al., 2004). A second source of chemodrive is from medullary raphe neurons that excite preBötC neurons with 5-hydroxytryptamine (5-HT) and Substance P. High concentrations of 5-HT and Substance P antagonists reduce preBötC activity in vitro and in situ (Ptak et al., 2009). Lesioning of the raphe leads to a transiently reduced CO2 response in vivo (Hodges et al., 2004). Additional excitatory drive to the VRC results from the cortical drive to breathe during wakefulness that is generated by supratentorial regions (Hugelin, 1986). Montandon et al. showed that the sedative effect of morphine decreased respiratory rate independent of the direct respiratory depressant effects of morphine on the VRC (Montandon et al., 2016). The neurotransmitters conveying this "wakefulness drive" have not yet been specified.

The present study focused on glutamatergic inputs, which appear essential for the preBötC and BötC function, as N-methyl-D-aspartate (NMDA) receptor antagonism in the BötC resulted in loss of rhythm in the in vivo rabbit preparation (Mutolo et al., 2005). Furthermore, NMDA receptor antagonism in the preBötC resulted in a significant reduction in inspiratory and expiratory duration and a decrease in peak phrenic activity (PPA) although not in apnea (Mutolo et al., 2005). In the in vitro preparation, α-amino-3-hydroxy-5-methyl-4-isoxazolepropionic acid (AMPA) receptor antagonism in the preBötC resulted in complete apnea (Funk et al., 1993). We have shown in the in vivo rabbit (Miller et al., 2017) and in vivo dog preparation (Zuperku et al., 2017, 2018) that medial parabrachial nucleus (PBN) activity has a significant impact, in particular on the expiratory-inspiratory phase switch. Zuperku et al. showed that stimulation of the medial PBN resulted in increased activity in preBötC pre-I neurons (Zuperku et al., 2017). In the rabbit, this area contains only non-respiratory modulated neurons (Miller et al., 2017), which suggests that they may be a source of tonic, glutamatergic drive to the preBötC.

To delineate the role of glutamatergic inputs to the individual components of the VRC we initially performed an exploratory study using grid-wise AMPA microinjections to generate a map of functionally identified subareas of the VRC and their spatial relation to each other. We then performed sequential injections of AMPA and NMDA receptor antagonists into the identified subareas, first the preBötC alone, and then sequential injections into the RTN, BötC and preBötC to determine the role of glutamatergic excitation in each area for respiratory rhythm generation.

2. Materials and methods

2.1. Surgical procedures

This research was approved by the subcommittee on animal studies of the Zablocki Veterans Affairs Medical Center, Milwaukee, Wisconsin, in accordance with provisions of the Animal Welfare Act, the Public Health Service Guide for the Care and Use of Laboratory Animals, and Veterans Affairs policy. Experiments were carried out on 29 adult (3–4 kg) New Zealand White rabbits of either sex. Animals were induced with 5 vol% sevoflurane via facemask and ventilated via tracheotomy with an anesthesia machine (Ohmeda CD, GE, Datex Ohmeda, Madison, WI). Anesthesia was maintained with 1.5–3% isoflurane. Inspiratory oxygen fraction, expiratory carbon dioxide concentration and expiratory isoflurane concentration were continuously displayed with an infrared analyzer (POET II, Criticare Systems, Waukesha, WI). Skin was infiltrated with lidocaine 1% before each skin incision. Femoral arterial and venous lines were used for blood pressure monitoring and infusion of solutions, respectively. Care was taken to increase anesthetic depth for any signs of “light anesthesia”, e.g., an increase in blood pressure or lacrimation. Lactated Ringer’s solution with 4 mcg/ml epinephrine was continuously infused at 1 ml/h. At this rate, the infusion did not result in appreciable changes in heart rate and blood pressure from baseline. Infusion rate was increased as needed to counteract or prevent hypotension in response to drug injections or from blood loss. The animal was maintained at 37.0 ± 0.5 °C with a warming blanket. The animal was placed in a stereotaxic frame (David Kopf Instruments, Tujunga, CA), and blunt precollicular decerebration with complete removal of the forebrain was performed through a parietal craniotomy. After decerebration isoflurane was either discontinued or continued at subanesthetic levels (0.3–0.4 vol%) for blood pressure control. Isoflurane concentration was not changed during the experimental protocol. The brainstem was exposed via occipital craniotomy and partial removal of the cerebellum. Animals were paralyzed with vecuronium (initially 1 mg/kg and redosed as needed) to avoid motion artifacts during neural/neuronal recording. Bilateral vagotomy was performed to achieve peripheral deafferentation to avoid interference of the mechanical ventilation with the underlying central respiratory rhythm and respiratory neuronal activity. The phrenic nerve was recorded with fine bipolar electrodes through a posterior neck incision. Throughout the experiment animals were ventilated with a hyperoxic gas mixture (FiO_2 0.6) to achieve functional denervation of the peripheral chemoreceptors and at mild hypercapnia (expiratory carbon dioxide: 45–55 mmHg) to ensure sufficient respiratory drive (i.e., to keep baseline phrenic activity stably above the apneic threshold). Blood pressure was maintained stable throughout the protocols by adjusting the intravenous infusion rate. At the end of the experiment, animals were euthanized with intravenous potassium chloride and the brainstem was removed and fixed for histological analysis.

2.2. Neuronal recording, microinjection procedures and measured variables

All neuronal recording and microinjection techniques have been well established by our research group and have been previously described in detail (Dogas et al., 1998; Krolo et al., 1999). In short, extracellular neuronal recordings were obtained using multibarrel micropipettes (20–40 μm tip diameter) consisting of three drug barrels and a recording barrel containing a 7 μm thick carbon filament. Barrels were filled with the glutamatergic agonist, α-amino-3-hydroxy-5-methyl-4-isoxazolepropionic acid (AMPA, 50 μM, 70 nl/ injection), the NMDA receptor antagonist d(–)-2-amino-5-phosphonopentanoic acid (D-AP5; 5 mM, 700 nl/ injection) and the non-NMDA receptor antagonist 2,3-dihydroxy-6-nitro-7-sulfamoyl-benzo[f]quinoxaline-2,3-dione (NBQX; 1 mM, 700 nl), which were dissolved in artificial cerebrospinal fluid. The microinjected volume was determined via height changes in the meniscus in the respective pipette barrel with a 100x monocular microscope and calibrated reticule (resolution ~3.5 nl). Respiratory neuronal discharge was recorded extracellularly from neuronal aggregates and individual neurons and classified by the temporal relationships relative to the phrenic neurogram. The neuronal and phrenic neural activity and pressure microejection marker signals were recorded using a digital acquisition system. These variables were also continuously displayed and recorded along with the phrenic neurogram, inspiratory time, expiratory time, discharge rate-meter, arterial blood pressure, airway carbon dioxide concentration on a computerized chart recorder (Powerlab/16SP; ADInstruments, Castle Hill, Australia). Before and after drug injection, steady-state conditions were obtained for respiratory parameters. Post experiment LabChart data was exported to SigmaPlot 11 (Systat Software, San Jose, CA) for data reduction, data plotting and statistical analysis. Between 10 and 50 consecutive respiratory cycles were averaged over 1–2 min with the

number of cycles dependent on the respiratory rate. Using the phrenic neurogram we determined peak phrenic activity (PPA), respiratory rate (RR) and inspiratory (TI) and expiratory (TE) duration. Since changes in PPA closely reflect changes in respiratory tidal volume but the absolute value does not correspond with the absolute tidal volume, (Eldridge FL 1976) PPA was normalized to control values for all calculations.

2.3. Histology

After conclusion of all experimental protocols, bilateral microinjections (140 nl) of fluorescent latex microspheres (Lumafluor.com; Red Retrobeads), diluted to 5% of the supplied concentration, were used to mark the injection sites for histological analysis. After euthanasia the brainstem was removed and submersed in paraformaldehyde (4%) fixative for 5 days and then stored in hypertonic sucrose (30% in PBS) with sodium azide (0.1%) before being flash frozen in isopentane and sectioned using a cryostat (Leica). Sequential coronal sections (of 20 μm thickness) were cut from the caudal edge of the inferior colliculi to 2-mm caudal to obex. For immunolabeling, free-floating sections were incubated in blocking solution (0.1 M phosphate buffered saline, 5% normal donkey serum, and 0.25% Triton X-100) for 1 h at room temperature. Sections were incubated in blocking solution with the following primary antibodies for 24 h at 4 °C: goat anti-ChAT (1:100, Millipore, AB144 P) and sheep anti-TH (1:500, Millipore, AB1542). The immunohistochemical staining patterns obtained with these antibodies were in agreement with the known expression patterns of the corresponding proteins, both at the cellular and subcellular level, supporting the specificity of these antibodies. Sections were incubated in the following secondary antibodies for 2 h at room temperature (all from Jackson ImmunoResearch): donkey anti-goat Alexa Fluor 488 (1:500), donkey anti-sheep Alexa Fluor 647 (1:500). Sections were counterstained with NeuroTrace 435/455 Blue Fluorescent Nissl Stain (1:25, Invitrogen, N21479), then mounted to glass slides using Fluoromount-G (Southern Biotech), coverslipped, and stored at 4 °C until imaging. A confocal laser-scanning microscope (Nikon C2+) at a 4x objective was used for all image acquisition. The settings for PMT, laser power, gain, and offset were identical between experimental groups. The atlas of Meessen and Olszewski was used for identification of relevant regions (Meessen and Olszewski, 1949).

2.4. Functional mapping of the ventral respiratory column (VRC) with AMPA injection

The locations of the major subareas of the VRC have been described before by neuron types and the respiratory response to injection of glutamate agonists for the rat (Chitravanshi and Sapru, 1999; Monnier et al., 2003), the cat (Solomon et al., 1999) and the rabbit (Bongianni et al., 2002; Mutolo et al., 2005). These studies provide a range of coordinates for the location of the preBötzinger complex (preBötC), the Bötzinger complex (BötC), and the ventral respiratory group (VRG) that are relative to obex. To aid our injection protocols, which at times require bilateral sequential injections into more than one subarea in short succession, we constructed a map of the VRC based on the changes in respiratory rate and PPA with AMPA injections, relative to the preBötC. By assuming that adjacent coordinates where AMPA injection causes a qualitatively similar response belong to the same subarea, this map also allowed us to gauge the dimensions of the BötC and preBötC. After successfully mapping the areas of interest, some of these animals were also used for the subsequent study protocols described below.

We inserted the microelectrode in a grid-wise fashion into the area between obex and the caudal end of the superior cerebellar peduncle. Step size was 0.5 mm medio-lateral and 0.47 mm rostro-caudal (i.e., a 0.5 mm step size corrected for a 20°- rostro-caudal angle between brainstem and stereotaxic frame). In areas where neuronal activity was encountered, we microinjected AMPA (50 μM, 70 nl) starting at the ventral end of the neuronal activity and then in 0.5 mm steps more dorsally until there was no neuronal activity detected or no more changes in the phrenic neurogram.

2.5. Injection protocol 1 - effect of glutamatergic disfacilitation in the preBötzinger Complex

For all protocols, the experimenters were not blinded to the experimental conditions. This protocol established the changes in respiratory pattern when endogenous glutamatergic excitation of the preBötC region was blocked by microinjections of the selective NMDA antagonist AP5 (5 mM, 700 nl) and the non-NMDA antagonist NBQX (1 mM, 700 nl). First, the preBötC region was identified bilaterally with grid-wise AMPA microinjections (see above). Then NBQX was microinjected bilaterally. Once changes in respiratory parameters had reached steady state (generally in less than three minutes), AP5 was microinjected bilaterally at the same coordinates. If the animal developed apnea, respiratory parameters were averaged over the last 10–20 breaths when a regular rhythm was still observed. To determine whether the order of antagonist injection influenced the magnitude of each effect, the antagonists were injected in reverse order in a separate set of animals. Only one protocol was performed per animal.

2.6. Injection protocol 2 - effect of glutamatergic disfacilitation in the Bötzinger Complex and preBötzinger Complex

This protocol established the changes in respiratory pattern resulting from disfacilitation of glutamatergic excitatory drive to the BötC region and subsequently from additional disfacilitation of the preBötC. The locations of the BötC and preBötC were functionally identified bilaterally with AMPA microinjection. Then NBQX (1 mM, 700 nl) was microinjected bilaterally into the BötC. After a 3-min wait, AP5 (5 mM, 700 nl) was injected bilaterally at the same coordinates. After 3–5 min, the same microinjection sequence was repeated in the preBötC. If the animal developed apnea, respiratory parameters were averaged over the last 10–20 breaths when a regular rhythm was still observed. Only one protocol was performed per animal.

2.7. Injection protocol 3 - effect of glutamatergic disfacilitation in the Retrotrapezoid Nucleus, the Bötzinger Complex and preBötzinger Complex

This protocol established the changes in respiratory pattern resulting from sequential disfacilitation of glutamatergic input into the RTN, BötC and preBötC areas, which were functionally identified with AMPA microinjections (see exploratory study). We performed bilateral sequential NBQX (1 mM, 700 nl) and AP5 (5 mM, 700 nl) microinjections into the RTN, then the BötC and finally preBötC as described above. Only one protocol was performed per animal.

2.8. Statistical analysis

Post-hoc data reduction, data plotting and statistical analysis of the pooled data were performed using SigmaPlot 11 (Systat Software, Richmond, CA). Sample size was based on published in vivo studies using similar protocols (Miller et al., 2017; Stucke et al., 2015). Data sets were tested for normal distribution (Shapiro-Wilk test). Statistical tests were performed on raw data except for peak phrenic activity (PPA), which is measured in arbitrary units and thus normalization to control is necessary to allow for comparison between animals. The effects of NBQX and AP5 injections on all respiratory parameters (RR, PPA, TI, and TE) in the preBötC were determined using one-way, repeated-measures analysis of variance (ANOVA) with Holm-Sidak correction for multiple comparisons for normally distributed data. The individual effects of NBQX and AP5 on respiratory parameters were compared using student's t-test. The effects of sequential NBQX and AP5 injections in the RTN, BötC, and preBötC were determined using two-way, repeated-measures ANOVA with injection area and drug as

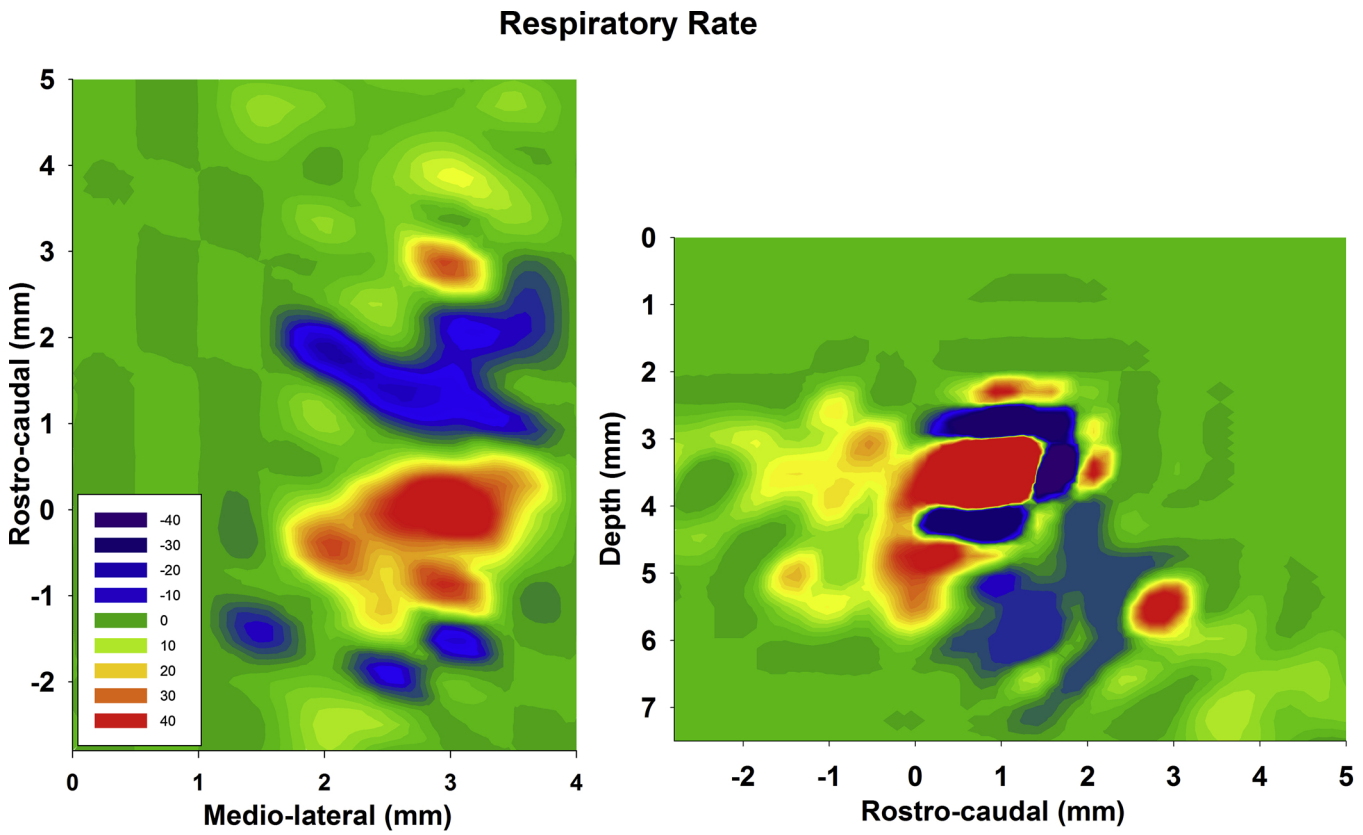

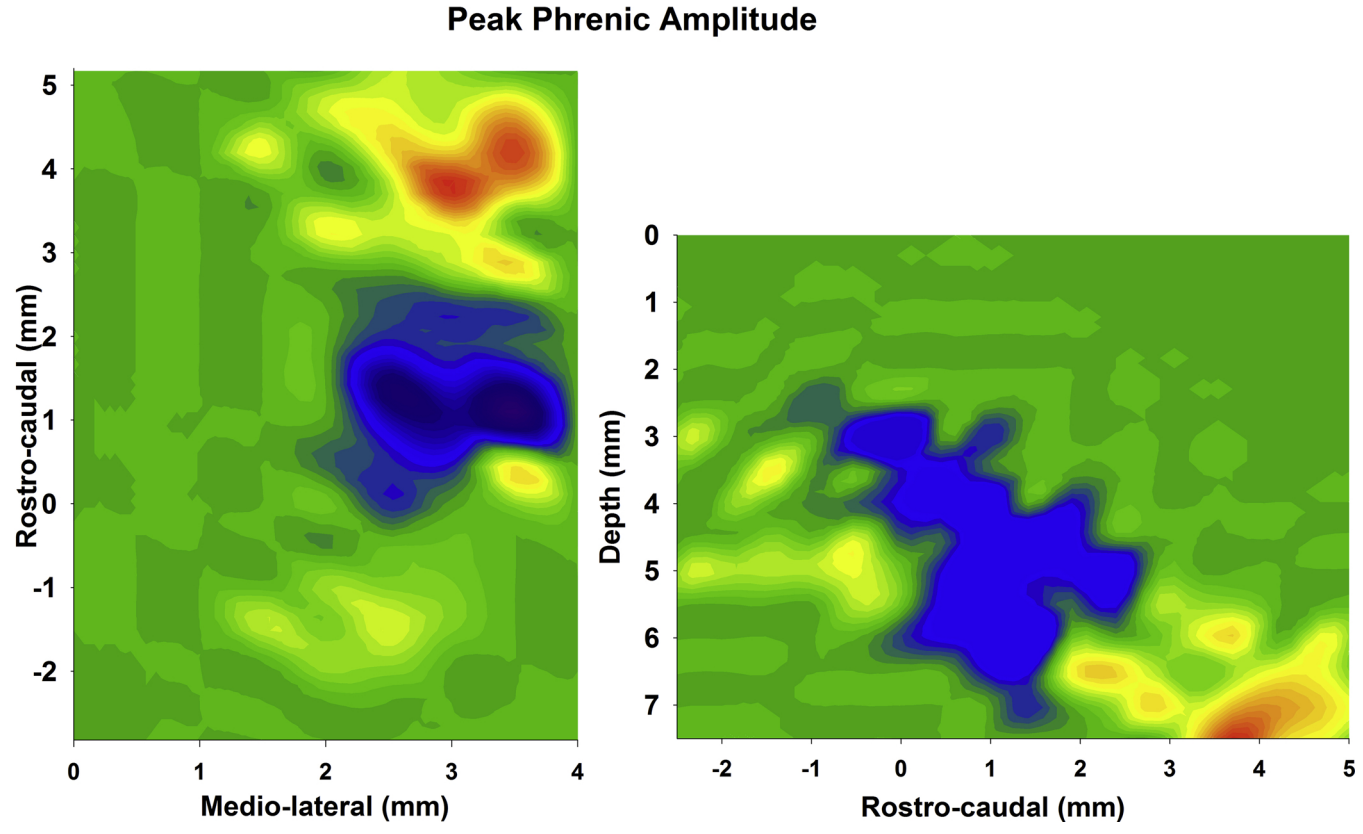

(caption on next page)

Fig. 1. Contour plots from 34 gridwise injections of AMPA (50 μM, 70 nl) in 18 animals indicate average percent change from baseline in respiratory rate (upper) and peak phrenic activity (lower). Left: presentation for the rostro-caudal and medio-lateral dimensions. Depicted is the greatest change at each coordinate independent of depth. Right: presentation for the rostro-caudal and dorso-ventral dimensions. Depicted is the greatest change at each coordinate independent of laterality. Step size was 0.5 mm medio-lateral and dorso-ventral and 0.47 mm (0.5 mm, corrected for an angle of 20° between brainstem and head holder) for rostro-caudal. The individual AMPA effects were aligned such that the preBötzinger Complex (preBötC) was always at 0 mm rostro-caudal. This placed the Bötzinger Complex ~1–1.5 mm rostral of the preBötC and the Retrotrapezoid Nucleus at ~4 mm rostral to the preBötC. Values are averaged for at least three injections per coordinate. Once no change was observed at a coordinate, grid-wise exploration was stopped and no change was assumed for all other coordinates more medial, lateral, dorsal or ventral than the ventral respiratory column. Scale: ≥ +50% (red) to -50% (blue) from baseline, green: no change.

factors and Holm-Sidak correction for multiple comparisons for normally distributed data and Friedman repeated measures ANOVA on ranks with Tukey test for pair-wise multiple comparisons for not normally distributed data. Differences were considered significant for $p < 0.05$. Values are expressed as mean ± SE.

3. Results

3.1. Functional mapping of the ventral respiratory column (VRC) with AMPA injection

Data was pooled from 34 unilateral maps in 18 animals (bilateral maps in 16 animals). There were at least three data points per coordinate. Not all areas were explored in every animal, but all maps included the preBötC. We designated the preBötC as the area of maximal AMPA-induced tachypnea and the BötC as the area of maximal AMPA-induced bradypnea (Fig. 1). The numerical values for the AMPA effect in each area are listed in Table 1. Neuronal activity in these areas matched the activity described in previous studies (Bongianni et al., 2002; Mutolo et al., 2005) with the preBötC mainly containing inspiratory neurons and the BötC containing mostly expiratory neurons, although we also recorded expiratory activity in the preBötC and inspiratory activity in the BötC in most animals. Smaller changes in respiratory rate and PPA were observed with AMPA injection into the VRG. We focused our AMPA injections on consistently identifying an area that contained a mix of inspiratory and expiratory neurons and where respiratory rate was increased. We called this area whose rostrocaudal location was at the level or slightly rostral to obex "rostral VRG" (rVRG). We also identified an area 0.5 mm rostral to the BötC where the respiratory rate was increased and a larger area ~1.5 mm rostral to the BötC where amplitude was increased. The latter area was close to the ventral surface and contained mainly non-respiratory modulated neurons although we occasionally observed inspiratory or expiratory neurons. Histology showed that this area was located towards the caudal end of the facial nucleus (Fig. 2). While the area of the RTN is not usually defined by its response to glutamate agonists, this location matches the area of the RTN with projections to the Kölliker-Fuse (KF) nucleus where NMDA application significantly increased PPA (Silva et al., 2016). The study protocols below used this area as the RTN.

The maximum AMPA response for rostro-caudal, medio-lateral and dorso-ventral coordinates was averaged for each area in the VRC. On average, the preBötC was located 1.8 ± 0.2 mm rostral to obex, 2.7 ± 0.1 mm lateral to midline and 4.9 ± 0.1 mm ventral to dorsal surface. Tachypnea was consistently observed at two to three levels (0.5 mm apart) in the dorso-ventral and mediolateral coordinates (Fig. 1). Significant tachypnea was also observed 0.47 and 0.94 mm caudal to the preBötC. The rVRG was located 1.5 ± 0.3 mm rostral to obex, 2.7 ± 0.1 mm lateral to midline and 4.5 ± 0.2 mm ventral to dorsal surface. At ~0.47 mm rostral to the preBötC AMPA injection caused an initial bradypnea and subsequent tachypnea or tachypnea with subsequent bradypnea suggesting that this was a transition area where AMPA was affecting neuronal populations in both the preBötC and the BötC. This response phenomenon has been described as "dysrhythmia" in the rat (Monnier et al., 2003). The BötC was located 2.9 ± 0.3 mm rostral to obex, 2.7 ± 0.1 mm lateral to midline and 5.5 ± 0.1 mm ventral to dorsal surface. Bradypnea was usually found over a distance of 0.94 mm rostro-caudally. These coordinates fall into the ranges of coordinates described by Bongianni (2002) and Mutolo (2005) (Bongianni et al., 2002; Mutolo et al., 2005). The RTN was located 5.0 ± 0.3 mm rostral to obex, 2.6 ± 0.2 mm lateral from midline and 6.6 ± 0.2 mm ventral to dorsal surface.

In eight animals, we injected fluorescent microspheres at the end of Injection Protocol 3 into the functionally identified RTN, BötC and preBötC (Fig. 2). Co-staining for Nissl substance, tyrosine hydroxylase and choline acetyltransferase confirmed that the antagonist injections were placed within the intended targets as shown relative to specific neuron types that define the anatomic location of key nuclei. The preBötC was located 1.2 ± 0.1 mm rostral to obex, ventral to the Nucleus Ambiguus (NA), medial to the adrenergic C1 group, and in one plane with the rostral end of the hypoglossal nucleus (Fig. 2, lower). The BötC was located 2.6 ± 0.2 mm rostral to obex, ventral to the Nucleus Ambiguus and medial to C1 (Fig. 2, middle). The RTN was located 4.6 ± 0.3 mm rostral to obex, ventral to the Facial Nucleus (7 N) and intermingled with the noradrenergic neurons of C1 (Fig. 2, top). We attribute the somewhat smaller distances from obex and in between the injected areas, compared to the coordinates for in vivo injections, with the shrinking of the tissue through the fixation process.

3.2. Injection protocol 1 - effect of glutamatergic disfacilitation in the preBötzinger Complex

Seven protocols were completed in adult rabbits receiving NBQX followed by AP5 injection in the preBötC. Univariate analysis of the effect of bilateral NBQX injection showed a small but significant increase in respiratory rate compared to baseline (27 ± 3 vs. 33 ± 3 breaths per minute, bpm, $p = 0.03$). This was due to a reduced inspiratory duration (1.11 ± 0.08 vs. 0.84 ± 0.07 s, $p < 0.001$) while expiratory duration was unchanged (1.27 ± 0.25 vs. 1.15 ± 0.19 s, $p > 0.05$). Normalized PPA was significantly reduced to 85 ± 7% of baseline ($p = 0.03$). Subsequent AP5 injection further increased respiratory rate up to 52 ± 3 bpm ($p < 0.001$), which was due to a reduced inspiratory duration (0.46 ± 0.07 s vs. 0.84 ± 0.07 s,

Table 1
Pooled data for AMPA response in the Retrotrapezoid Nucleus, Bötzinger Complex and preBötzinger Complex.

Respiratory Variables	RTN (n = 10)	BötC (n = 21)	preBötC (n = 34)	rVRG (n = 19)
Inspiratory Time (s)	−9.1 ± 1.14%	30.62 ± 9.54%	−21.32 ± 4.3%	−11.08 ± 3.96 %
Expiratory Time (s)	−11.07 ± 1.96%	40.04 ± 9.38%	−25.03 ± 12.91%	−32.03 ± 2.96 %
Respiratory rate (bpm)	18.96 ± 9.54%	−22.21 ± 3.29%	65.42 ± 12.53%	33.9 ± 6.32%
Peak Phrenic Amplitude (%)	12.93 ± 1.94%	−24.32 ± 3.43%	−14.08 ± 3.23%	6.6 ± 3.49 %

Data presented as mean ± SE of the percentage change compared to baseline. n = number of measurements.

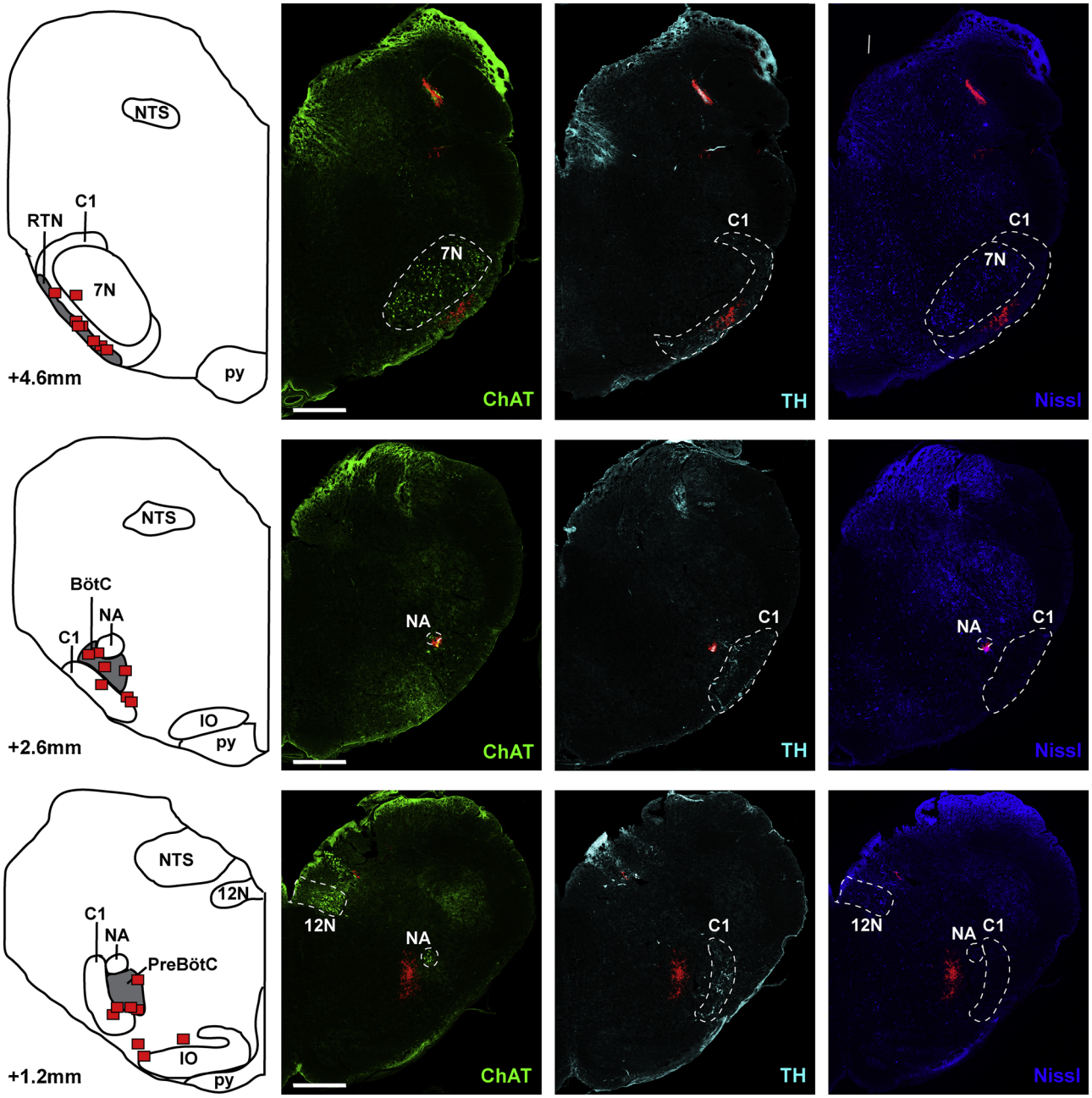

Fig. 2. Location of the preBötzinger Complex (preBötC), Bötzinger Complex (BötC) and Retrotrapezoid Nucleus (RTN) as identified by injection of fluorescent latex microspheres in eight rabbits. The left panel shows diagrammatic hemisections of the brainstem at each rostro-caudal level with the individual injection sites superimposed in red squares. The right panels show the corresponding hemisections from one animal with immunoreactivity for choline acetyltransferase (ChAT), tyrosine hydroxylase (TH) and Nissl substance. Red microspheres mark the area of injection of the test substances in Protocol 3. NTS: Nucleus of the Solitary Tract; NA: Nucleus Ambiguus; IO: Inferior Olive; py: pyramidal tract; 12N: Nucleus Hypoglossus; 7 N: Nucleus facialis; C1: adrenergic C1 group. Bar = 1 mm.

$p < 0.001$). AP5 did not significantly reduce expiratory duration compared to NBQX, however, the expiratory duration was significantly reduced compared to control (0.72 ± 0.06 s vs. 1.27 ± 0.25 s, $p = 0.031$). Normalized PPA was significantly reduced to 33 ± 4% of baseline ($P < 0.001$) (Fig. 3).

Six protocols were completed in adult rabbits with reverse order of antagonist injection, i.e., receiving AP5 followed by NBQX microinjection in the preBötC. Univariate analysis of the effect of bilateral AP5 injection into the preBötC showed a significant increase in respiratory rate compared to baseline (61 ± 12 vs. 33 ± 6 bpm, $p = 0.003$). This was due to a reduced inspiratory duration (0.73 ± 0.21 vs. 1.25 ± 0.26 s, $p = 0.010$) while expiratory duration was not significantly reduced (0.75 ± 0.36 vs. 1.03 ± 0.31 s, $p = 0.14$). Normalized PPA was significantly reduced to 63 ± 10% of baseline ($P < 0.001$). Subsequent injection of NBQX caused a small but not significant increase in respiratory rate (70 ± 12 bpm vs. 61 ± 12 bpm, $p = 0.18$) and small but not significant decreases in inspiratory duration (0.52 ± 0.08 s vs. 0.73 ± 0.21 s, $p = 0.177$) or expiratory duration (0.57 ± 0.21 s vs. 0.75 ± 0.36 s, $p = 0.22$) compared to AP5 injection. However, expiratory duration was significantly reduced compared to baseline ($p = 0.024$). Normalized PPA was further reduced to 44 ± 17% of baseline ($P = 0.031$). At the end of the experiments, 10 out of 13 animals became apneic within 20 s of the second antagonist injection (see Fig. 3 A, second trace). The three remaining animals showed a significant decrease in inspiratory and expiratory duration and PPA with loss of regular rhythm in two animals,

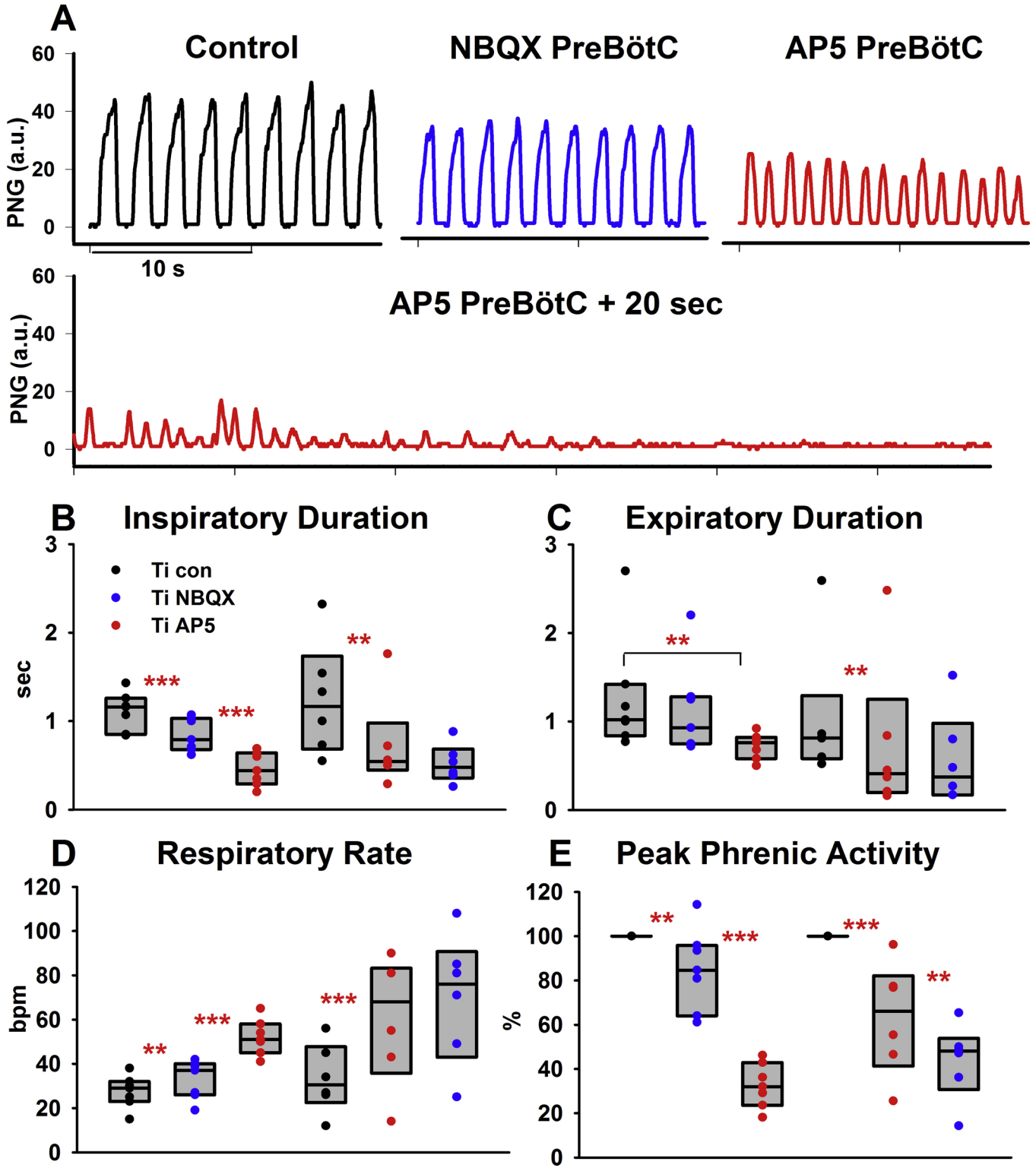

Fig. 3. Disfacilitation of glutamatergic drive to the preBötzinger Complex (preBötC). A: Phrenic neurogram (PNG) tracings show that bilateral microinjection of NBQX and subsequently AP5 caused tachypnea with decreased peak phrenic activity (PPA), which was followed by apnea. B-E: Pooled data for the sequential, bilateral injection of NBQX and AP5 in 13 animals. In 7 animals, NBQX (blue) was injected first (left-hand side of each panel), in 6 separate animals, AP5 (red) was injected first (right-hand side of each panel). Peak phrenic activity was normalized to control. See text for details. Box plots (median, 25–75% range) plus individual data points. *: $p < 0.05$, **: $p < 0.01$, ***: $p < 0.001$.

however no complete apnea.

Comparison of the effects of NBQX vs. AP5 injection yielded the following insights: 1) The magnitude of the respective effects of NBQX and AP5 appears to be independent of the order in which they were injected. NBQX microinjection increased respiratory rate by 20 ± 4% when injected before AP5 and 24 ± 12% when injected after AP5 ($p = 0.84$). Similarly, the PPA decreased by 15 ± 7% when NBQX was injected before vs. 31 ± 5% when injected after AP5 ($p = 0.11$).

Respiratory rate increased 78 ± 19% when AP5 was microinjected before vs. 66 ± 15% after NBQX ($p = 0.602$), with a decrease in PPA by 37 ± 10% when injected before vs. 61 ± 5% after NBQX ($p = 0.05$). 2) The combined effect produced by AP5 and NBQX is similar to the sum of their separate effects, which suggests an additive rather than synergistic contribution of both receptor subtypes to the glutamatergic drive to the neurons of the preBötC. The sum of the individual increase in respiratory rate after NBQX and AP5 injections was 96 ± 18%, which was not statistically different from the combined effect of NBQX plus AP5 (100 ± 19.7%) or AP5 plus NBQX (116 ± 19%)($P = 0.8$). Similarly, the sum of individual decrease in PPA after NBQX and AP5 injections was -51 ± 12%, which was not significantly different from the combined effect of NBQX plus AP5 (-67 ± 4%) or AP5 plus NBQX (-56 ± 7%)($P = 0.2$). 3) Fig. 3 illustrates that AP5 injection caused greater changes in respiratory parameters than NBQX injection. AP5 elicited a greater respiratory rate increase compared to NBQX whether administered before NBQX (66 ± 15% vs. 20 ± 4%, $p = 0.01$) or after NBQX (78 ± 19% vs. 24 ± 12%, $p = 0.03$). This suggests that most of the endogenous glutamatergic input to the preBötC under the prevailing experimental conditions (hyperoxic hypercapnia) in our in vivo preparation is NMDA-receptor mediated.

3.3. Injection protocol 2 - effect of glutamatergic disfacilitation in the Bötzinger Complex and preBötzinger Complex

Five protocols were completed in adult rabbits receiving NBQX followed by AP5 injection in the BötC. Disfacilitation of the BötC reduced inspiratory duration from 0.77 ± 0.07 s to 0.45 ± 0.05 s ($n = 5$, $p = 0.003$) and expiratory duration from 0.91 ± 0.14 s to 0.37 ± 0.04 s ($p = 0.003$), resulting in an increase in respiratory rate from 37 ± 4 bpm to 75 ± 5 bpm ($p < 0.001$). Normalized PPA did not significantly change (92 ± 4% vs. 100%, $p = 0.058$). Subsequent disfacilitation of the preBötC did not cause an additional decrease in inspiratory duration (0.43 ± 0.01 s, $p = 0.33$). The decrease in expiratory duration to 0.16 ± 0.04 s was not significant ($p = 0.63$), however, respiratory rate significantly increased to 103 ± 4 bpm ($p = 0.009$). Normalized PPA decreased to 71 ± 6% ($p < 0.001$), and all animals developed a significant degree of tonic inspiratory activity (Fig. 4, B1 and B2).

Fig. 4 illustrates the difference between the PNG responses due to disfacilitation of the preBötC alone in one animal (Fig. 4A) vs. disfacilitation of the preBötC following prior disfacilitation of the BötC in a different animal (Fig. 4B). Disfacilitation of the preBötC alone resulted in an increase in breathing rate and a gradual, marked reduction in PPA, which maintained a silent expiratory phase. In contrast, with prior disfacilitation of the BötC, disfacilitation of the preBötC resulted in a marked increase in breathing rate and a gradual, but significant, reduction in the phasic PNG with an increase in expiratory phase activity, eventually ending in tonic inspiratory activity (Fig. 4 B1 & B2). An analysis of the effects of disfacilitation on the PPA and phase timing can be obtained from the ratio of PPA to timing parameters as shown in Fig. 4C. In the preBötC, glutamatergic disfacilitation altered PPA much more than respiratory rate. Inspection of TI and TE vs. PPA plots show that as disfacilitation progressed, the decreases in TI appear to be offset by increases in TE with the net result of little change in breathing rate (Fig. 4C, left). Prior disfacilitation of the BötC had a markedly different effect on the breathing rate-PPA plot (Fig. 4C, right), i.e., both variables changed in a linear relationship. Both TI and TE continued to decrease as PPA decreased, i.e., the combined disfacilitation of the BötC and preBötC had a greater impact on the reduction of TE.

3.4. Injection protocol 3 - effect of sequential glutamatergic disfacilitation in the RTN, the Bötzinger Complex and preBötzinger Complex

Seven protocols were completed in adult rabbits receiving NBQX followed by AP5 injection in the RTN. Univariate analysis showed that there was no significant change in respiratory rate ($p = 0.49$), TI ($p = 1.0$), TE ($p = 0.3$) or PPA ($p = 0.77$) after NBQX and AP5 injections. Subsequently, animals were injected with NBQX and AP5 in the BötC and preBötC.

Statistical analysis showed that the effect of BötC and preBötC disfacilitation was not different whether the RTN had ($n = 7$) or had not ($n = 5$, Protocol 2) been injected before. We thus pooled the data for disfacilitation of the BötC and preBötC from both protocols to increase the power of the analysis. The pooled data ($n = 12$, Table 2) again show that disfacilitation of the BötC significantly decreased inspiratory and expiratory duration ($p < 0.001$), which increased respiratory rate ($p < 0.001$). Subsequent bilateral injection in the preBötC did not result in any further decrease in inspiratory duration ($p = 0.56$) while expiratory duration decreased even more ($p = 0.003$, Fig. 5). In all but one animal, the respiratory pattern was lost and tonic phrenic nerve activity ensued. The remaining animal showed a decrease in PPA by 40% and an increase in respiratory frequency from 26 to 81 bpm.

In chloralose/urethane anesthetized rabbits with an expiratory PCO_2 of 28–32 mmHg, Mutolo et al. (2005) found that maximum disfacilitation of the BötC produced tonic, non-rhythmic phrenic activity, which we did not observe in our study with expiratory PCO_2 of ~50 mmHg in decerebrated rabbits. Accordingly, in a subset of 8 rabbits, we performed microinjections into the BötC at expiratory PCO_2 of ~30 mmHg. With maximum disfacilitation, rhythmic activity persisted in 4 of 8 rabbits. In the other 4 rabbits, microinjections of the glutamatergic antagonists resulted in a loss of regular rhythm and tonic inspiratory activity similar to Mutolo et al. (2005) results. When expiratory PCO_2 was increased to ~50 mmHg, the phrenic activity in two rabbits became rhythmic again, and in the other two animals, some respiratory rhythm recovered but never became completely regular. The data from the latter two rabbits were not included in the pooled data.

4. Discussion

This study used sequential disfacilitation/ block of glutamatergic inputs to the functionally identified BötC and preBötC to investigate the role of endogenous glutamatergic drive in respiratory pattern generation in the VRC in vivo. We found that in our adult, decerebrate rabbit preparation 1) disfacilitation of the preBötC produced a striking tachypnea via decreases in inspiratory and expiratory duration with a very large decrease in peak phrenic activity (PPA), resulting in apnea; 2) disfacilitation of the BötC resulted in a significant decrease in inspiratory and expiratory duration with minimal decrease in PPA; 3) disfacilitation of the RTN did not have any significant effect on the respiratory rhythm, and 4) disfacilitation of both, the BötC and preBötC revealed tonic excitatory inputs to inspiratory premotor neurons.

Microinjections of AMPA showed distinctly different responses in respiratory rate and peak phrenic amplitude delineating the anatomical boundaries of the BötC and preBötC regions (Fig. 1). While a mixture of various types of inspiratory and expiratory neurons has been found within these regions, certain types predominate in each region. Thus, disfacilitation of these neurons with glutamatergic antagonists can be expected to have different effects on the respiratory pattern dependent on the role of the affected neurons in phase timing and respiratory drive.

4.1. Glutamatergic inputs to the preBötzinger Complex

Glutamatergic inputs are essential for the preBötC to function as the respiratory rhythm and pattern generator because disfacilitation of these inputs caused apnea in our in vivo preparation. These data are consistent with a model where respiratory phase duration is determined by reciprocal inhibition since glutamatergic disfacilitation of the preBötC resulted in a parallel decrease in inspiratory and expiratory

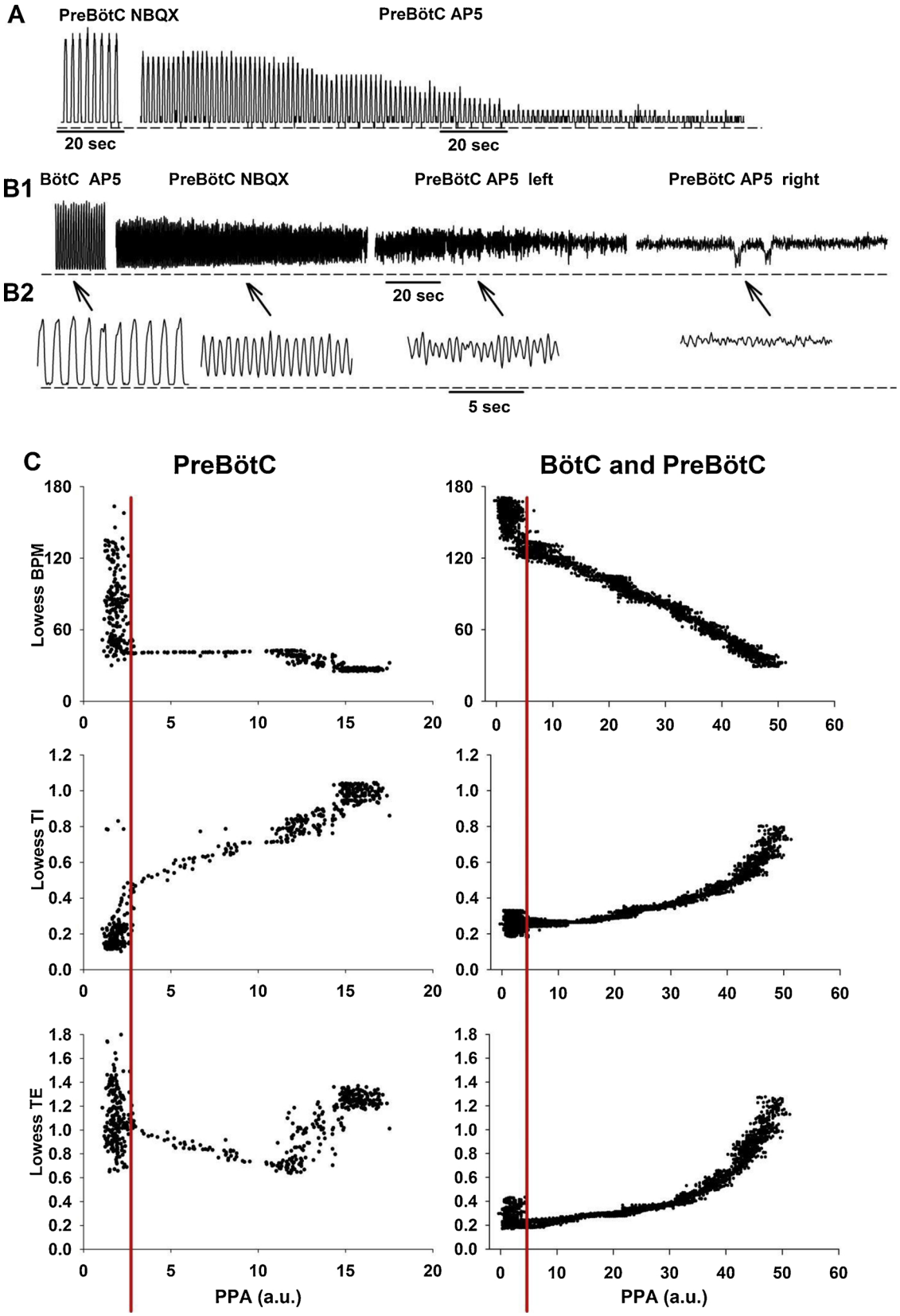

(caption on next page)

duration and PPA (Stuth et al., 2005a, b). Below a certain threshold, characterized by low PPA (Figs. 3A and 4 C, left of red line), regular rhythm is lost and the respiratory effort resembles low-amplitude inspiratory "burstlets" of short duration, interrupted by expiratory phases of irregular duration before apnea ensued. In this context, it is interesting that the duration of an inspiratory cycle did not decrease below ~400 −500 ms before the regular rhythm, i.e., inspiratory and expiratory cycles of consistent duration, was lost. This was observed with

Fig. 4. A: Phrenic neurogram showing the effect of glutamatergic disfacilitation of the preBötzinger Complex (preBötC) in one animal. Shown are clips after bilateral injection of NBQX (left) and after subsequent bilateral injection of AP5 (right). There was significant shortening of inspiratory (TI) and expiratory (TE) duration and decrease in peak phrenic amplitude (PPA) until apnea ensued. There was no tonic activity. B1: Phrenic neurogram showing the effect of glutamatergic disfacilitation of the Bötzinger Complex (BötC) and preBötC in a different animal. Shown are clips after bilateral injection of NBQX and AP5 into the BötC, after subsequent bilateral injection of NBQX into the preBötC, after AP5 injection into the left preBötC and after AP5 injection into the right preBötC. TI, TE and PPA significantly decreased until rhythm was lost, however, significant tonic activity persisted. B2: Enlarged detail of the indicated time points. C: To determine whether PPA changed in parallel with respiratory phase timing we plotted the breath-by-breath data for respiratory rate (BPM), TI and TE from the displayed sections in 4 A and 4B. Data were smoothed using Lowess function. PPA for BötC injections was calculated as the amplitude of the phasic activity above tonic activity. The decrease in PPA correlated with the change in respiratory phase timing, in particular with TI. As PPA decreased below a certain threshold (red line) regular rhythm was lost. For the pooled data for Protocols 1–3, we averaged only data to the right of the threshold.

Table 2
Pooled data for sequential glutamatergic disfacilitation in the Retrotrapezoid Nucleous, Bötzinger Complex and preBötzinger Complex.

Respiratory Variables	Retrotrapezoid Nucleus (n = 7)			Bötzinger Complex (n = 12)			preBötzinger Complex (n = 12)	
	Baseline	NBQX	AP5	Baseline	NBQX	AP5	NBQX	AP5
Inspiratory Time (s)	0.77 (0.05)	0.77 (0.05)	0.77 (0.04)	0.77 (0.03)	0.63 (0.03)	0.48 (0.03)	0.44 (0.03)	0.47 (0.03)
Expiratory Time (s)	1.15 (0.15)	1.14 (0.15)	1.17 (0.14)	1.06 (0.11)	0.85 (0.08)	0.45 (0.05)	0.30 (0.05)	0.22 (0.03)
Respiratory Rate (bpm)	33 (3)	33 (3)	32 (3)	35 (2)	42 (2)	68 (4)	91 (11)	88 (5)
Peak Phrenic Amplitude (%)	100	101 (1)	94 (6)	100	103 (3)	95 (6)	88 (4)	72 (4)

Data presented as mean ± SE.

and without prior disfacilitation of the BötC. A similar minimal inspiratory duration was also observed by Mutolo et al. (Mutolo et al., 2005). It is possible that the reinforcing effect produced by the excitatory synaptic connections among inspiratory neurons (Ezure, 1990) was reduced below the critical level needed to generate a coordinated inspiratory burst (Butera et al., 1999).

A mechanistic explanation for the effects of disfacilitation observed in the present study is given by the hypothetical model of Fig. 6. The preBötC region contains a mixture of pre-I, I-aug and I-dec neurons as well as some E-dec neurons (Ezure, 1990; Guyenet and Wang, 2001; Krolo et al., 2005; Schwarzacher et al., 1995; Zuperku et al., 2018). Tonic excitation of all types of neurons is required for their proper function. Reciprocal inhibition between the I-dec and E-dec neurons plays a key role in controlling the duration of their respective phases, and a reduction in tonic excitation leads to decreases in both inspiratory and expiratory duration and their respective peak firing rates (Fig. 6C, also see model responses in (Stuth et al., 2005a, b). In addition, disfacilitation of the pre-I and I-aug neurons would decrease their peak firing rates resulting in an additional decrease in PPA.

Our results extend those obtained by Mutolo et al. (Mutolo et al., 2005) in in vivo, chloralose-urethane anesthetized rabbits, which showed that glutamate antagonism caused a decrease in inspiratory duration, expiratory duration and PPA but could not achieve complete apnea with one glutamate receptor subtype antagonist (CNQX or AP5) alone. We showed that both receptor subtypes needed to be blocked to obtain complete apnea with a greater contribution of the NMDA receptor subtype. In contrast, glutamatergic inputs to the preBötC in neonatal rat medullary slice preparations were solely mediated by AMPA receptors (Funk et al., 1993), although under conditions of high synaptic glutamate concentrations, Morgado-Valle et al. (Morgado-Valle and Feldman, 2004) showed that a significant portion of the glutamate-elicited excitatory postsynaptic current was mediated by NMDA receptors.

4.2. Glutamatergic input to the Bötzinger Complex

The BötC contains in its majority E-aug and E-dec neurons and in addition a small number of I-dec, pre-I, and I-aug neurons (Schwarzacher et al., 1995; Zuperku et al., 2018). It is located in the area ventromedial to the retrofacial nucleus but does not form a morphologically distinct nucleus. Augmenting-E neurons connect abundantly to neurons in the BötC/preBötC/VRG area as well as to the dorsal respiratory group and the pons (Ezure, 1990). These neurons inhibit inspiratory neurons in the dorsal respiratory group (DRG), the VRG and phrenic motoneurons. They also inhibit expiratory neurons in the cVRG and the vagal motonucleus. Therefore, E-aug neurons of the BötC exert widespread inhibitory influence on medullary respiratory neurons.

Intermingled with E-aug neurons are E-dec neurons, which are less abundant (Bianchi and Barillot, 1982; Ezure and Manabe, 1988). These neurons are propriobulbar and have extensive projections to the BötC/preBötC/VRG including the E neurons of the cVRG and DRG (Ezure, 1990). Unlike post-inspiratory neurons, E-dec neurons discharge throughout the entire expiratory phase. They inhibit propriobulbar and bulbospinal inspiratory neurons and are the only neurons which are inhibitory and fire at the time of the inspiratory-expiratory phase transition (Ezure, 1990). This finding supports the idea that the E-dec neurons are inhibitory and play an important role in the inspiratory-expiratory phase transition.

In the present study, we identified the BötC by transient bradypnea following microinjection of AMPA (Fig. 1: dark blue, 1–2.5 mm rostral to the tachypneic preBötC, red, centered at 0 mm rostro-caudal). Disfacilitation of this region by NBQX and AP5 resulted in a marked reduction in both inspiratory and expiratory duration. However, PPA was not reduced, which was different from glutamatergic disfacilitation of the preBötC region. We propose that a reduction in the activity of the E-dec/I-dec phase-timing neurons may be responsible for the decreases in inspiratory and expiratory duration (Fig. 6B). Since there are fewer inspiratory neurons in this region compared with the preBötC region, any reduction in their discharge may only have had a minor effect on the PPA. Disfacilitation of the BötC E-aug and E-dec neurons, which play an important role in the maintenance of the silent expiratory phase of the inspiratory bulbospinal neurons and phrenic motoneurons led to a significant reduction in expiratory duration (Fig. 5C). Still, there was no or minimal tonic phrenic activity during the expiratory phase after disfacilitation of the BötC alone, suggesting that E-dec neurons in the preBötC region continued to provide expiratory phase inhibition to maintain the silent expiratory phase of the PNG. However, when E-dec neurons of both regions were disfacilitated, expiratory phase inhibition was lost and continued tonic glutamatergic excitation of the inspiratory bulbospinal neurons (Krolo et al., 2000) produced a continuous, uninterrupted discharge (Fig. 4, B1, and Fig. 6D).

Similarly to Mutolo et al., (Mutolo et al., 2005) our data suggest that the role of the BötC in rhythm generation depends on the level of drive to the pattern generator. At low PCO_2 (~30 mmHg), glutamatergic disfacilitation resulted in a loss/ near loss of rhythm with tonic

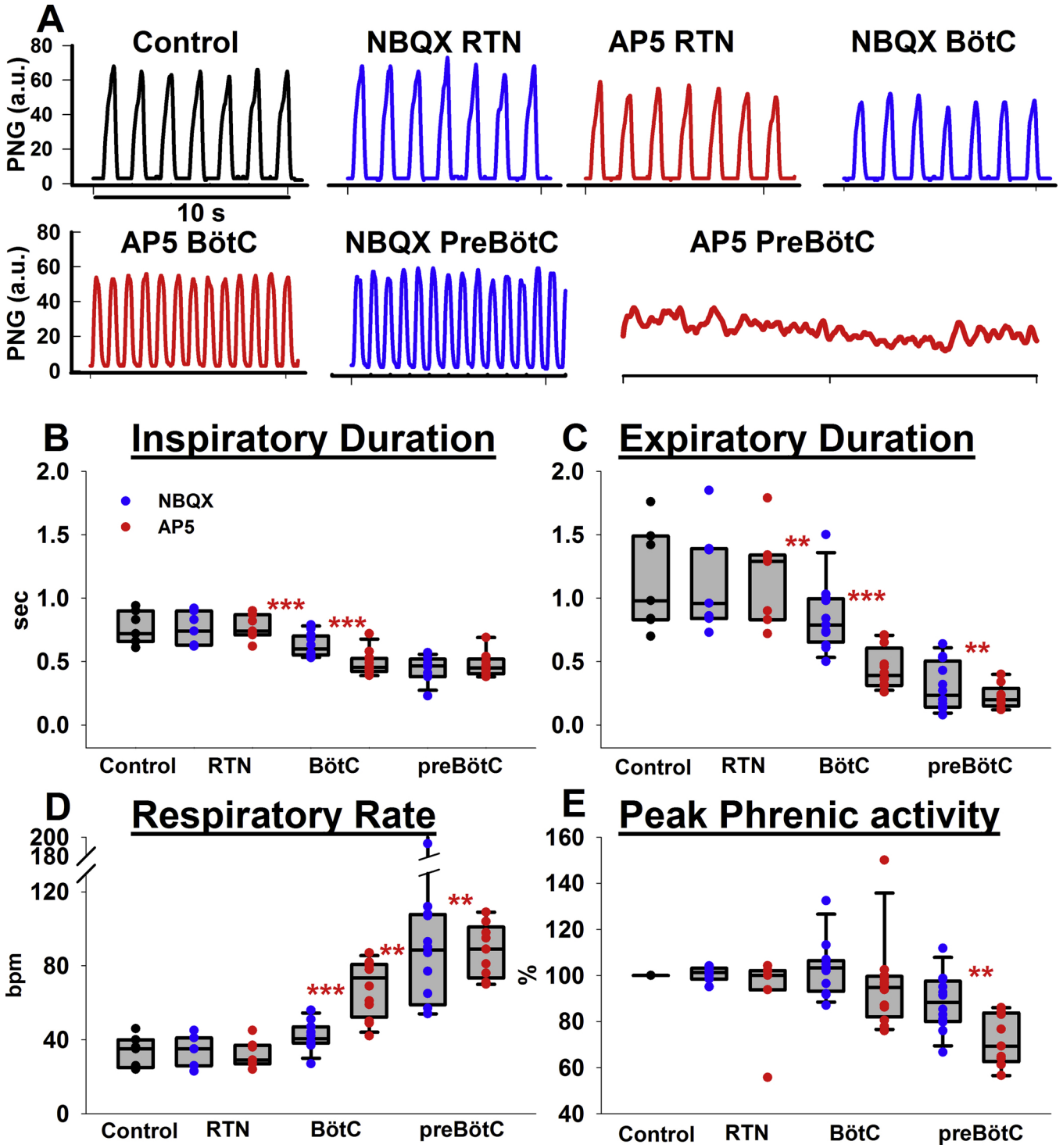

Fig. 5. Sequential disfacilitation of glutamatergic drive to the Retrotrapezoid Nucleus (RTN), Bötzinger Complex (BötC) and preBötzinger Complex (preBötC). A: Phrenic neurogram (PNG) tracings show that bilateral NBQX and AP5 injections into the RTN did not have a significant effect on rate; injections into the BötC increased respiratory rate, and subsequent injections into the preBötC caused tonic inspiratory activity that was interrupted by expiratory activity at irregular intervals. Peak phrenic activity was normalized to control. B-E: Pooled data for NBQX and AP5 injections into the RTN, BötC and preBötC in 7 and into the BötC and preBötC in 5 animals. See text for details. Box plots (median, 25–75% range) plus individual data points. *: $p < 0.05$, **: $p < 0.01$, ***: $p < 0.001$.

inspiratory activity in half of the animals. We suspect that we did not see loss of rhythm in all animals because the apneic threshold in our decerebrate preparation may be lower than with the profound sedation used by Mutolo et al. (Mutolo et al., 2005). In those animals that lost rhythm during hypocapnia, regular rhythm returned promptly when CO_2 was increased to ~50 mmHg and normalized completely in two animals. This is again similar to Mutolo et al. (Mutolo et al., 2005), where rhythm returned with hypercapnia (~60 mmHg) (Mutolo et al., 2005). The peak discharge frequency of respiratory-related neurons is directly related to the level of PCO_2 (Cohen, 1968; Stuth et al., 1994). Thus, at low PCO_2 levels, peak neuronal activities are lower than at normocapnia and their synaptic interactions would be expected to be much less robust. We suggest that the disfacilitation of BötC E-neurons would markedly reduce their ability to inhibit medullary I neurons and

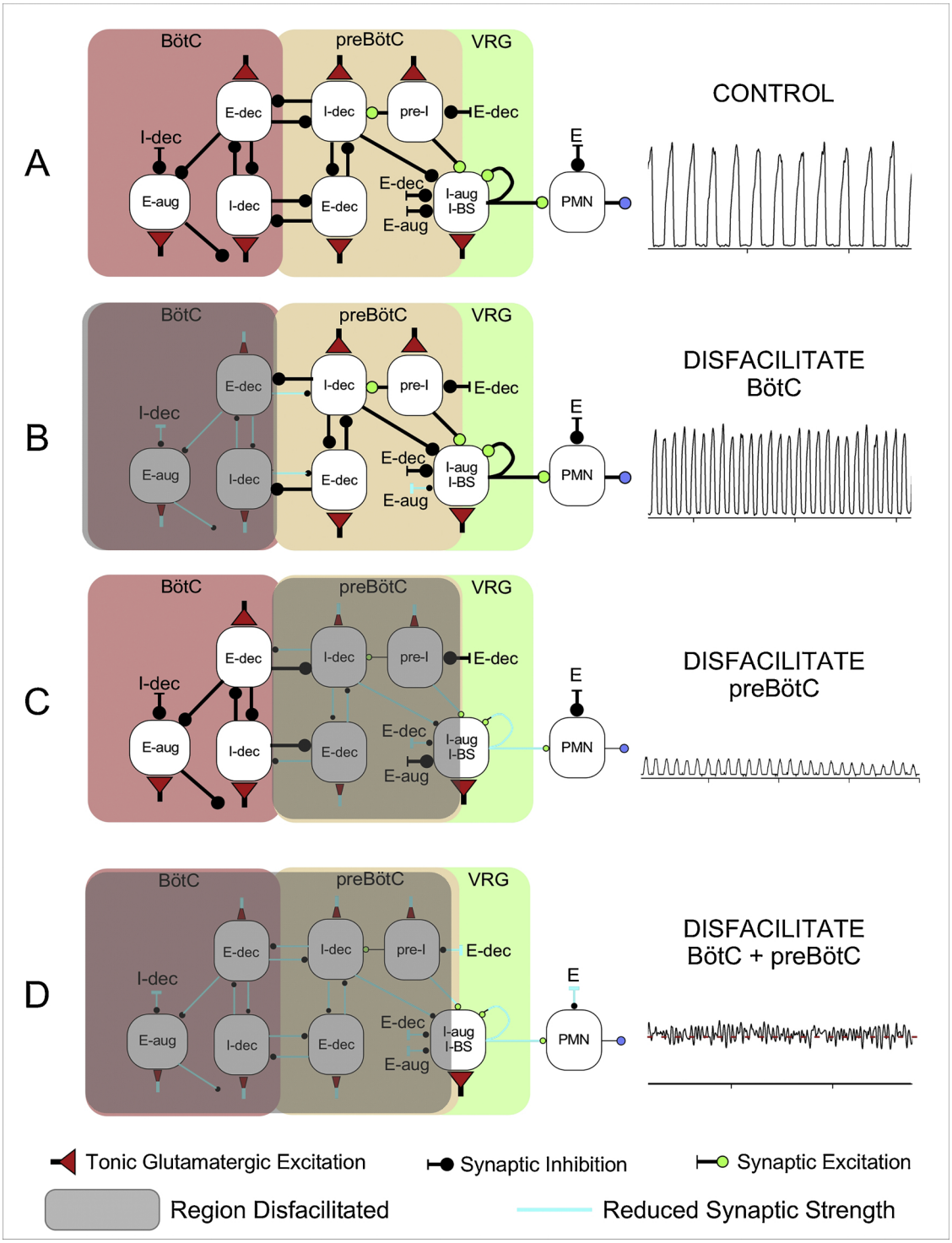

Fig. 6. Schematic of a hypothetical model for the effects of regional glutamatergic disfacilitation on the respiratory pattern. A: Control network configuration, B: Disfacilitation of the Bötzinger Complex (BötC), C: Disfacilitation of the preBötzinger Complex (preBötC), and D: Disfacilitation of both regions. Depicted are the inspiratory (I) and expiratory (E) neuronal discharge types located in the respective region, which are believed to underlie the mechanism of reciprocal inhibition. Color of the buttons indicates the type of synaptic connection with red: tonic glutamatergic excitation, green: (phasic) glutamatergic excitation, black: synaptic inhibition. aug: augmenting; dec: decrementing; VRG: ventral respiratory group; PMN: phrenic motoneuron; BS: bulbospinal neuron. Shaded region: disfacilitated neurons with reduced synaptic transmission. See Discussion for details.

phrenic motoneurons. Increasing PCO_2 levels would facilitate the activity of the E-DEC neurons caudal to the BötC, which would then generate a sufficient level of inhibition and produce the silent E-phase.

4.3. Glutamatergic input to the Retrotrapezoid Nucleus

We included the RTN in our brainstem map and in parts of our injection protocols because changes in chemodrive can affect respiratory rate and PPA (Mulkey et al., 2004; Silva et al., 2016), as does stimulation with NMDA (Silva et al., 2016) or optogenetic stimulation

(Abbott et al., 2011). The RTN contains a group of CO_2-sensitive neurons with tonic discharge pattern (Mulkey et al., 2004) that are Phox2B positive, located close to the ventral surface and send glutamatergic projections to multiple respiratory-related areas in the VRC and pons (Bochorishvili et al., 2012; Guyenet and Bayliss, 2015). We functionally identified two areas at ~0.5 mm rostral and 1–1.5 mm rostral of the BötC where AMPA injection caused an increase in respiratory rate. In analogy to other studies, we chose for our injection protocols the more rostral area, which also showed a prominent, prolonged increase in PPA (Fig. 1, lower left, red-orange region). Post mortem histological analysis showed that this area was indeed very close to the ventral surface and towards the caudal pole of the facial nucleus. Interestingly, we did not observe any significant changes in rhythm or PPA with glutamatergic disfacilitation of this area. It is possible that our injection volume was not large enough to disfacilitate a sufficiently large area of the RTN. Alternatively, under our experimental conditions (FiO_2 0.6, PCO_2 50, vagotomy) glutamatergic drive to the RTN may have been much reduced so that disfacilitation did not cause significant changes in RTN function.

4.4. Methodological considerations

4.4.1. Injection volumes

In order to functionally locate the BötC and preBötC areas, studies using microinjection have focused on injecting the smallest effective amounts to avoid confounding effects on adjacent VRC subareas. We found in pilot experiments that a typical response to a glutamate agonist could be achieved with relatively small volumes (35–70 nl) with a maximal effect achieved within 30 s and recovery to baseline respiratory rate in < 3 min. The Appendix illustrates that the minimum effective concentration for AMPA to achieve a receptor effect was present over a radius of 400–500 µm from the micropipette (Figure C). Since microinjection grid spacing was 500 µm, some overlap occurred between injection sites. However, dependent on the subpopulation of neurons predominantly stimulated by the injection (Schwarzacher et al., 1995; Zuperku et al., 2018) the effects of AMPA injection on the respiratory pattern were remarkably consistent, and adjacent microinjections could produce responses in opposite directions.

In contrast to AMPA injections, which only aimed for a qualitative effect, our pilot data indicated that much larger injection volumes (700 nl) of glutamate antagonists were often required to achieve *maximal* effects shortly after injection (~3 min). Applying the same model, a minimum effective tissue concentration of AP5 and NBQX was present shortly after injection over a spherical radius of 1000–1200 µm around the pipette tip. Projected on Fig. 1, a 1000 µm radius would again suggest an overlap of the diffusion areas between adjacent BötC and preBötC injections. However, the qualitatively distinctly different effects of BötC and preBötC injections suggest that this overlap did not affect a sufficient number of neurons in the adjacent area to confound the results.

Considering animal/ brainstem size, our microinjection volume probably matched the ~110 nl volumes recent studies used to inject the BötC and preBötC in 300–400 g rats (Janczewski et al., 2013; Marchenko et al., 2016). Interestingly, the quality and magnitude of the effects we observed resembled those obtained in a similar rabbit model with much smaller volumes (30–50 nl) but higher antagonist concentrations (20 mM), where maximal effects occurred after 6–10 min (Mutolo et al., 2005). This is reflected in our model where prolonged diffusion time allows the spread of a small fraction of the pipette concentration over a much larger radius than that of the initial injection volume (Appendix figure B).

Whenever we did not achieve a complete loss of respiratory rhythm the injections were likely placed slightly off target and did not cover a sufficient number of neurons. The necessary area of drug diffusion may be larger than previously acknowledged and possibly exceeds the spread of concomitantly injected, particulate dye (Janczewski et al., 2013; Marchenko et al., 2016).

4.4.2. Decerebrate preparation

The complexity of our experimental setup requires a paralyzed, insensate and unconscious preparation. We use decerebration to avoid general anesthetic effects on glutamatergic and/ or GABAergic receptor function and thus respiratory control. Decerebration results in a very regular respiratory rhythm resembling slow-wave sleep (Burke et al., 2015; Souza et al., 2018). While slow-wave sleep does not reduce minute ventilation or CO2 response in the rat (Burke et al., 2015), in the in vivo dog model in our lab, decerebration raised the apneic threshold (Stuth et al., 2000). This was likely due to the loss of suprapontine excitatory inputs (Hugelin, 1986). Montandon et al. (2016) showed in rats that the loss of cortical arousal from morphine depressed respiratory rate in addition to the direct depressant effects of morphine on the brainstem (Montandon et al., 2016). We attempt to compensate for the loss of suprapontine respiratory drive by using moderate hypercapnia during our experimental protocols.

4.4.3. CO_2 level

We have described above how the difference in end tidal CO_2 affected the results observed with disfacilitation of the BötC, which is consistent with other studies (Mutolo et al., 2005). Although the physiological, normocapnic PCO_2 in the rabbit is closer to 30 mmHg, it is difficult to gauge what PCO_2 would be appropriate to reflect the role of the BötC in the conscious animal since deeper planes of anesthesia as well as decerebration raise the apneic threshold. Since our laboratory also focuses on anesthetic and opioid effects on respiratory control and increased PCO_2 levels are required to maintain respiratory rhythm throughout these protocols, we elected to use our standard levels of moderate hypercapnia, and take into account that the elevated PCO_2 may be a confounder of the physiological function we observe.

4.4.4. VRG subareas

While the preBötC and BötC are defined through distinctive respiratory rhythm changes with glutamate agonist injections, the nomenclature for the subareas of the VRG is less consistent. Bongianni undertook detailed mapping of the VRG by neuronal discharge type in in vivo rabbits (Bongianni et al., 2002). In rostro-caudal order, they distinguished between the “inspiratory VRG”, which was just caudal to the preBötC and contained mostly inspiratory neurons, the “transitional VRG” containing a mix of inspiratory and expiratory neurons and the “caudal VRG” containing expiratory neurons. Glutamatergic disfacilitation of the inspiratory VRG with high AP5 concentrations resulted in a small decrease in respiratory rate and subsequent apnea from a decrease in PPA. They saw no effect in the other areas. Monnier et al. determined in adult rats in vivo that the “rostral VRG”, located immediately caudal to the preBötC, contained mostly inspiratory neurons (Monnier et al., 2003). DLH injection caused bradypnea just caudal to the preBötC but no other effects caudal to this area. In our preparation, functional mapping with AMPA injections showed significant tachypnea over two and sometimes three rostro-caudal injection sites (0.47 and 0.94 mm apart), often at more than one depth level, which we interpreted as the full extent of the preBötC (Fig. 1, upper, red-orange). Caudal to this, we observed mild bradypnea and mild tachypnea, suggesting that this population of inspiratory and expiratory neurons could still affect respiratory rate. Without performing any more detailed investigation, we labeled this area the “rostral VRG” (Fig. 1, upper, caudal to ~-1.5 mm).

5. Conclusion

We showed in an adult, in vivo decerebrate rabbit model that regular respiratory rhythm depends on glutamatergic drive to the preBötC that is primarily mediated by NMDA, but also by AMPA receptors. Sequential disfacilitation first of the BötC and then of the preBötC

revealed an important contribution of the BötC to maintenance of the expiratory phase through direct inhibition of inspiratory VRG neurons, which appears to be closely coordinated with the rhythm generated in the preBötC. The importance of BötC-derived inhibition of inspiratory activity for the maintenance of respiratory rhythm may depend on the level of drive to the respiratory network.

Acknowledgements

The authors thank Jack Tomlinson (Biologic Laboratory Technician) for excellent technical assistance and Andrew Williams (Engineering Technician) for his outstanding support with the experimental setup (both Medical College of Wisconsin, Milwaukee, Wisconsin). This work was supported by the NIH (RO1-GM112960, Dr. Stucke) and VA merit award (I01BX000721, Dr. Zuperku).

Appendix A

Model to estimate drug spread after microinjection of glutamate agonists and antagonists into the ventral respiratory column (VRC). We used microinjection volumes of 70 nl to functionally identify VRC subareas and volumes of 700 nl to achieve maximal effects of glutamate antagonist injections into each VRC subarea. According to Nicholson (Nicholson, 1985), a 70 nl microinjection produces an initial spherical volume with a radius of 429 μm ($r = 104.3*V^{1/3}$ μm). A 700 nl microinjection produces an initial spherical radius of 923 μm. This calculation takes into account that in an isotropic medium extracellular space is 21% of the tissue volume, which results in a larger spherical radius as the injected volume fills the smaller space between cells. In addition, the diffusion path is tortuous, and this effect is accounted for by the tortuosity factor (λ), which has been found to be ~1.6 (Nicholson, 1985; Nicholson and Syková, 1998). The rate of diffusion is inversely proportional to the square root of the molecular weight (MW).

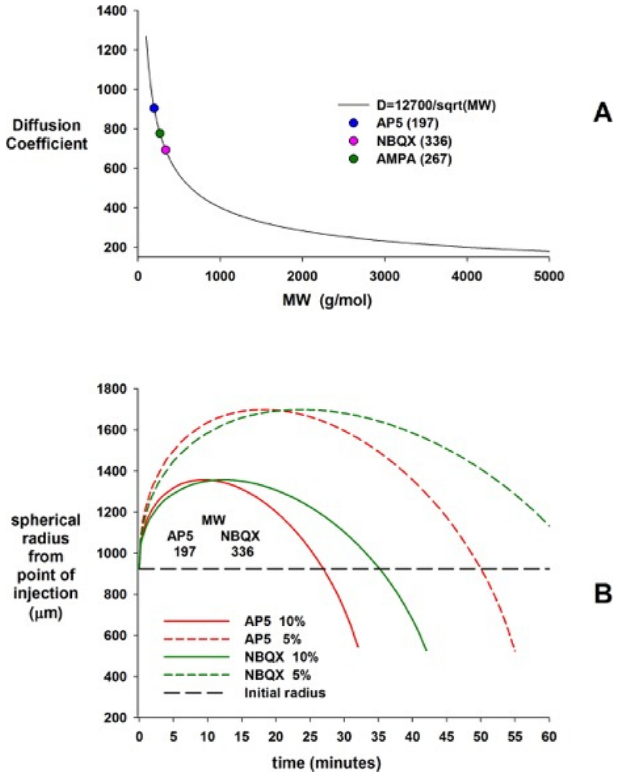

A: A curve fit to a plot of the diffusion coefficient, D vs. MW for data from experimental determined values is D ≅12700/sqrt(MW). Because of the tortuosity, the effective diffusion coefficient is given by $D^* = D/\lambda^2$. **B**: Substances with higher MW diffuse more slowly, however, the maximal radius of a drug concentration from point of injection is similar for different MW. Small fractions of the original pipette concentration (here: 5 and 10%) reach much greater areas than the initial injection volume (black horizontal line) albeit with significant delay. In other words, provided adequate diffusion time even small injection volumes can affect a large radius of cells if the injected drug concentration is 10- or 20 times higher than the minimum concentration required for the receptor effect.

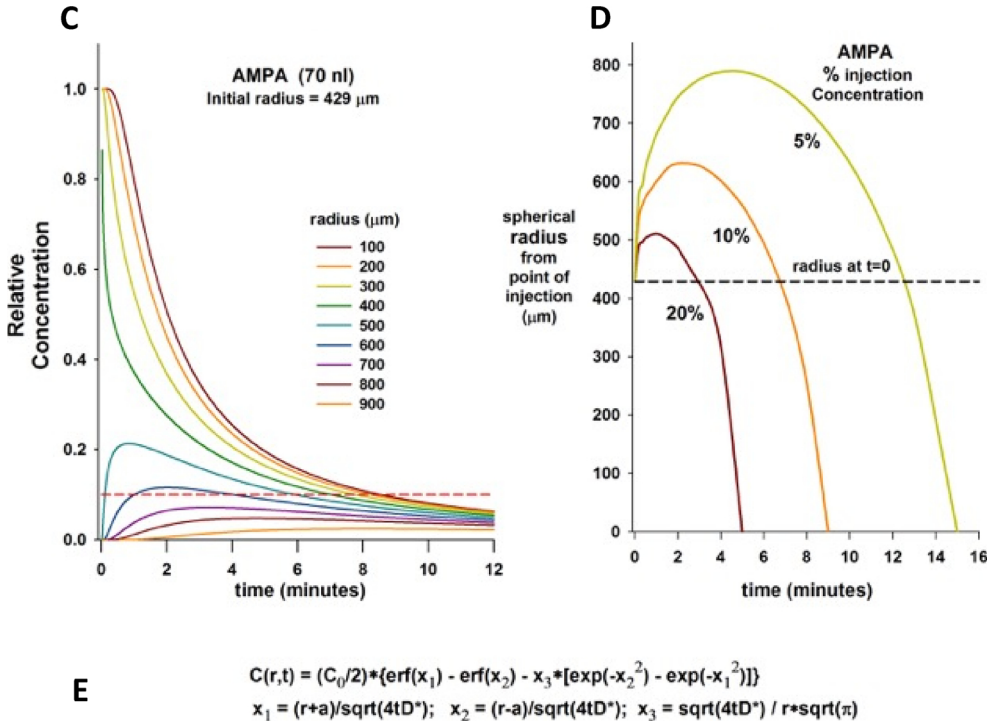

C: Tissue concentrations of AMPA at increasing radius from the pipette tip after injection of a 70 nl bolus. The pipette concentration (1.0) reaches an initial radius of 429 μm. Tissue concentration declines rapidly close to the pipette tip. Red dotted line: tissue concentration of 5μM with pipette concentration 50μM. The minimum effective concentration (MEC) for AMPA to increase neuronal discharge frequency when injected in close proximity to a single VRG neuron was 10μM (personal observation based on recordings of canine respiratory neurons in vivo by EJ Zuperku, 2004). In our study, maximal AMPA effect was observed within 30 s and respiratory rate returned to control levels in < 3 min suggesting that a MEC of AMPA was present at a radius of 400–500 μm from the pipette tip. **D**: Small fractions of the pipette concentration can be found in a significantly greater radius around the injection site, but only several minutes after the injection. **E**: Diffusion curves were created with concentration (C) as a function of time (t) and radius from center of the injection site (r); erf: error function; a: initial injected volume radius; D: diffusion coefficient.

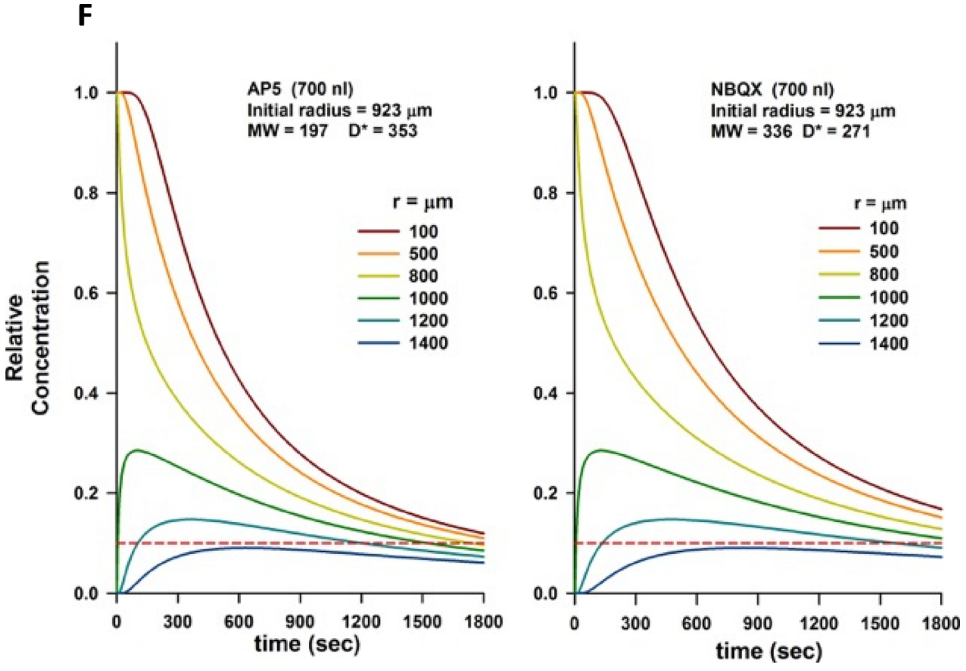

F: Tissue concentrations of AP5 and NBQX at increasing radius from the pipette tip after injection of a 700 nl bolus. The pipette concentration (1.0) reaches an initial radius of 923 μm. Tissue concentration declines rapidly close to the pipette tip. Without clear reference data we assumed a MEC for AP5 and NBQX of 10% of the pipette concentration (red dotted line). This concentration is present at a radius of 1000–1200 μm around the pipette tip. Maximum drug effect in our preparation was reached within 3 min of injection.

References

Abbott, S.B., Stornetta, R.L., Coates, M.B., Guyenet, P.G., 2011. Phox2b-expressing neurons of the parafacial region regulate breathing rate, inspiration, and expiration in conscious rats. J. Neurosci. 31, 16410–16422.

Bianchi, A.L., Barillot, J.C., 1982. Respiratory neurons in the region of the retrofacial nucleus: pontile, medullary, spinal and vagal projections. Neurosci. Lett. 31, 277–282.

Bochorishvili, G., Stornetta, R.L., Coates, M.B., Guyenet, P.G., 2012. Pre-Botzinger complex receives glutamatergic innervation from galaninergic and other retrotrapezoid nucleus neurons. J. Comp. Neurol. 520, 1047–1061.

Bongianni, F., Mutolo, D., Carfi, M., Pantaleo, T., 2002. Respiratory responses to ionotropic glutamate receptor antagonists in the ventral respiratory group of the rabbit. Pflugers Arch. 444, 602–609.

Bongianni, F., Mutolo, D., Cinelli, E., Pantaleo, T., 2010. Respiratory responses induced by blockades of GABA and glycine receptors within the Botzinger complex and the pre-Botzinger complex of the rabbit. Brain Res. 1344, 134–147.

Burke, P.G., Kanbar, R., Basting, T.M., Hodges, W.M., Viar, K.E., Stornetta, R.L., Guyenet, P.G., 2015. State-dependent control of breathing by the retrotrapezoid nucleus. J. Physiol. 593, 2909–2926.

Butera Jr, R.J., Rinzel, J., Smith, J.C., 1999. Models of respiratory rhythm generation in the pre-Botzinger complex. II. Populations of coupled pacemaker neurons. J. Neurophysiol. 82, 398–415.

Chitravanshi, V.C., Sapru, H.N., 1999. Phrenic nerve responses to chemical stimulation of the subregions of ventral medullary respiratory neuronal group in the rat. Brain Res. 821, 443–460.

Cohen, M.I., 1968. Discharge patterns of brain-stem respiratory neuronsin relation to carbon dioxide tension. J. Neurophysiol. 31, 142–165.

Cui, Y., Kam, K., Sherman, D., Janczewski, W.A., Zheng, Y., Feldman, J.L., 2016. Defining preBotzinger complex rhythm- and pattern-generating neural microcircuits in vivo. Neuron 91, 602–614.

Dogas, Z., Krolo, M., Stuth, E.A., Tonkovic-Capin, M., Hopp, F.A., McCrimmon, D.R., Zuperku, E.J., 1998. Differential effects of GABAA receptor antagonists in the control of respiratory neuronal discharge patterns. J. Neurophysiol. 80, 2368–2377.

Stuth, E., Zuperku, E., Stucke, A., 2005a. Central effects of general anesthesia. Lung Biol.Health Dis. 202, 571.

Stuth, E.A.E., Zuperku, E.J., Stucke, A.G., 2005b. Central effects of general anesthesia. In: Denham, S., Ward, A.D., Teppema, Luc J. (Eds.), Pharmacology and Pathophysiology of the Control of Breathing. Tayor and Francis Group, Boca Raton, FL, pp. 571–652.

Ezure, K., 1990. Synaptic connections between medullary respiratory neurons and considerations on the genesis of respiratory rhythm. Prog. Neurobiol. 35, 429–450.

Ezure, K., Manabe, M., 1988. Decrementing expiratory neurons of the Botzinger complex. Exp. Brain Res. 72, 159–166.

Funk, G.D., Greer, J.J., 2013. The rhythmic, transverse medullary slice preparation in respiratory neurobiology: contributions and caveats. Respir. Physiol. Neurobiol. 186, 236–253.

Funk, G.D., Smith, J.C., Feldman, J.L., 1993. Generation and transmission of respiratory oscillations in medullary slices: role of excitatory amino acids. J. Neurophysiol. 70, 1497–1515.

Guyenet, P.G., Bayliss, D.A., 2015. Neural control of breathing and CO2 homeostasis. Neuron 87, 946–961.

Guyenet, P.G., Wang, H., 2001. Pre-Bötzinger neurons with preinspiratory discharges "in vivo" express NK1 receptors in the rat. J. Neurophysiol. 86, 438–446.

Hodges, M.R., Klum, L., Leekley, T., Brozoski, D.T., Bastasic, J., Davis, S., Wenninger, J.M., Feroah, T.R., Pan, L.G., Forster, H.V., 2004. Effects on breathing in awake and sleeping goats of focal acidosis in the medullary raphe. J. Appl. Physiol. (Bethesda, Md.: 1985) 96, 1815–1824.

Hugelin, A., 1986. Forebrain and midbrain influence on respiration. Handbook of Physiology, Sect 3.

Janczewski, W.A., Tashima, A., Hsu, P., Cui, Y., Feldman, J.L., 2013. Role of inhibition in respiratory pattern generation. J. Neurosci. 33, 5454–5465.

Kam, K., Worrell, J.W., Janczewski, W.A., Cui, Y., Feldman, J.L., 2013. Distinct inspiratory rhythm and pattern generating mechanisms in the preBotzinger complex. J. Neurosci. 33, 9235–9245.

Krolo, M., Stuth, E.A., Tonkovic-Capin, M., Dogas, Z., Hopp, F.A., McCrimmon, D.R., Zuperku, E.J., 1999. Differential roles of ionotropic glutamate receptors in canine medullary inspiratory neurons of the ventral respiratory group. J. Neurophysiol. 82, 60–68.

Krolo, M., Stuth, E.A., Tonkovic-Capin, M., Hopp, F.A., McCrimmon, D.R., Zuperku, E.J., 2000. Relative magnitude of tonic and phasic synaptic excitation of medullary inspiratory neurons in dogs. Am. J. Physiol. Regul. Integr. Comp. Physiol. 279, R639–R649.

Krolo, M., Tonkovic-Capin, V., Stucke, A., Stuth, E., Hopp, F., Dean, C., Zuperku, E., 2005. Subtype composition and responses of respiratory neurons in the pre-Botzinger region to pulmonary afferent Inputs in dogs. J. Neurophysiol. 93, 2674–2687.

Lindsey, B.G., Segers, L.S., Shannon, R., 1987. Functional associations among simultaneously monitored lateral medullary respiratory neurons in the cat:II. Evidence for inhibitory actions of expiratory neurons. J. Neurophysiol. 57 (4), 1101–1117.

Marchenko, V., Koizumi, H., Mosher, B., Koshiya, N., Tariq, M.F., Bezdudnaya, T.G., Zhang, R., Molkov, Y.I., Rybak, I.A., Smith, J.C., 2016. Perturbations of respiratory rhythm and pattern by disrupting synaptic inhibition within pre-botzinger and Botzinger Complexes. eNeuro 3.

Meessen, H., Olszewski, J., 1949. A cytoarchitectonic atlas of the rhombencephalon of the rabbit. A Cytoarchitectonic Atlas of the Rhombencephalon of the Rabbit.

Miller, J.R., Zuperku, E.J., Stuth, E.A.E., Banerjee, A., Hopp, F.A., Stucke, A.G., 2017. A subregion of the parabrachial nucleus partially mediates respiratory rate depression from intravenous remifentanil in young and adult rabbits. Anesthesiology 127, 502–514.

Monnier, A., Alheid, G.F., McCrimmon, D.R., 2003. Defining ventral medullary respiratory compartments with a glutamate receptor agonist in the rat. J. Physiol. 548, 859–874.

Montandon, G., Cushing, S.L., Campbell, F., Propst, E.J., Horner, R.L., Narang, I., 2016. Distinct cortical signatures associated with sedation and respiratory rate depression by morphine in a pediatric population. Anesthesiology 125, 889–903.

Morgado-Valle, C., Feldman, J.L., 2004. Depletion of substance P and glutamate by capsaicin blocks respiratory rhythm in neonatal rat in vitro. J. Physiol. (Lond.) 555, 783–792.

Mulkey, D.K., Stornetta, R.L., Weston, M.C., Simmons, J.R., Parker, A., Bayliss, D.A., Guyenet, P.G., 2004. Respiratory control by ventral surface chemoreceptor neurons in rats. Nat. Neurosci. 7, 1360–1369.

Mutolo, D., Bongianni, F., Nardone, F., Pantaleo, T., 2005. Respiratory responses evoked by blockades of ionotropic glutamate receptors within the Botzinger complex and the pre-Botzinger complex of the rabbit. Eur. J. Neurosci. 21, 122–134.

Nicholson, C., 1985. Diffusion from an injected volume of a substance in brain tissue with arbitrary volume fraction and tortuosity. Brain Res. 333, 325–329.

Nicholson, C., Syková, E., 1998. Extracellular space structure revealed by diffusion analysis. Trends Neurosci. 21, 207–215.

Ptak, K., Yamanishi, T., Aungst, J., Milescu, L.S., Zhang, R., Richerson, G.B., Smith, J.C., 2009. Raphe neurons stimulate respiratory circuit activity by multiple mechanisms via endogenously released serotonin and substance P. J. Neurosci. 29, 3720–3737.

Rybak, I.A., O'Connor, R., Ross, A., Shevtsova, N.A., Nuding, S.C., Segers, L.S., Shannon, R., Dick, T.E., Dunin-Barkowski, W.L., Orem, J.M., Solomon, I.C., Morris, K.F., Lindsey, B.G., 2008. Reconfiguration of the pontomedullary respiratory network: a computational modeling study with coordinated in vivo experiments. J. Neurophysiol. 100, 1770–1799.

Schwarzacher, S.W., Smith, J.C., Richter, D.W., 1995. Pre-Botzinger complex in the cat. J. Neurophysiol. 73, 1452–1461.

Silva, J.N., Lucena, E.V., Silva, T.M., Damasceno, R.S., Takakura, A.C., Moreira, T.S., 2016. Inhibition of the pontine Kölliker-Fuse nucleus reduces genioglossal activity elicited by stimulation of the retrotrapezoid chemoreceptor neurons. Neuroscience 328, 9–21.

Solomon, I.C., Edelman, N.H., Neubauer, J.A., 1999. Patterns of phrenic motor output evoked by chemical stimulation of neurons located in the pre-Botzinger complex in vivo. J. Neurophysiol. 81, 1150–1161.

Souza, G., Kanbar, R., Stornetta, D.S., Abbott, S.B.G., Stornetta, R.L., Guyenet, P.G., 2018. Breathing regulation and blood gas homeostasis after near complete lesions of the retrotrapezoid nucleus in adult rats. J. Physiol. 596, 2521–2545.

Stucke, A.G., Miller, J.R., Prkic, I., Zuperku, E.J., Hopp, F.A., Stuth, E.A., 2015. Opioid-induced respiratory depression is only partially mediated by the preBotzinger complex in young and adult rabbits in vivo. Anesthesiology 122, 1288–1298.

Stuth, E.A.E., Tonkovic-Capin, M., Kampine, J.P., Bajic, J., Zuperku, E.J., 1994. Dose-dependent effects of halothane on the carbon dioxide responses of expiratory and inspiratory bulbospinal neurons and the phrenic nerve activities in dogs. Anesthesiology 81, 1470–1483.

Stuth, E.A., Krolo, M., Stucke, A.G., Tonkovic-Capin, M., Tonkovic-Capin, V., Hopp, F.A., Kampine, J.P., Zuperku, E.J., 2000. Effects of halothane on excitatory neurotransmission to medullary expiratory neurons in a decerebrate dog model. Anesthesiology 93, 1474–1481.

Zuperku, E.J., Stucke, A.G., Hopp, F.A., Stuth, E.A., 2017. Characteristics of breathing rate control mediated by a subregion within the pontine parabrachial complex. J. Neurophysiol. 117, 1030–1042.

Zuperku, E.J., Stucke, A.G., Krolikowski, J.G., Tomlinson, J., Hopp, F.A., Stuth, E.A., 2018. Inputs to medullary respiratory neurons from a pontine subregion that controls breathing frequency. Respir. Physiol. Neurobiol.